First steps with HLLMHD and PP reconstruction: Part III

by *O. Steiner, P. Rajaguru,* and *G. Vigeesh*

This is a continuation of part I and II of this report. In this third part we report results obtained with a cool stellar model—model `d3t40g45mm00n01` with $T_{\rm eff} = 4000$ K and $\log g = 4.5$, provided by Matthias Steffen. This model has, like the model with $T_{\rm eff} = 5000$ K (`d3t50g45mm00n04`), n1 $\times$ n2 $\times$ n3 $= 140 \times 140 \times 141$ grid cells. The size of the box is 4.702 Mm $\times$ 4.702 Mm $\times$ 1.2269 Mm. The $\tau = 1$ level is at a height of about 0.74 Mm from the bottom. The grid cells have a horizontal width of 33.8 km and a vertical extent varying from 11.75 km in the bottom part of the convection zone to ≈ 7.9 km in the top part of the convection zone and down to 6.78 km in the top part of the box. As in part II, we examine the total radiative output at the top boundary as a function of time and some horizontally averaged quantities as a function of height and of time. The initial model consists of relaxed convection as computed with the Roe solver and Van Leer reconstruction. The initial magnetic field (if not set zero) is homogeneous and vertical with a strength of 50 G.

job	solver	reconstr.	N_ordCT	$\nu_{\rm art.}$	$B_{\rm init}$ [G]	initial model	$t_{\rm end}$ [s]
job_d3t40g45mm00n01_Roe	Roe	VanLeer	—	0.0	—	d3t40g45mm00n01.1320402	3606
job_d3t40g45mm00n01_B0	HLLMHD	PP	2	0.0	$B_z = 0$	d3t40g45mm00n01_B0	7209
job_d3t40g45mm00n01_v50	HLLMHD	PP	2	0.0	$B_z = 50$	d3t40g45mm00n01_v50	7206
job_d3gt57g44n59_B0	HLLMHD	PP	2	0.0	$B_z = 0$	d3gt57g44n59_B0	3603
job_d3gt57g44n59_v50	HLLMHD	PP	2	0.0	$B_z = 50$	d3gt57g44n59_v50	3603
job_d3t50g45mm00n04_dt	HLLMHD	PP	2	0.0	$B_z = 0$	d3t40g45mm00n01_B0	3601
job_d3t50g45mm00n04_RK	HLLMHD	PP	2	0.0	$B_z = 0$	d3t40g45mm00n01_B0	3605

Table 1: Model simulations. job_d3t50g45mm00n04_dt was computed with a maximum time step of 0.1 s. job_d3t50g45mm00n04_RK was computed with Runge Kutta 2nd order time integration.

In addition, Matthias has provided a solar model (`d3gt57g44n59`), which is comparable in size and spatial resolution to the stellar models. This model has n1 $\times$ n2 $\times$ n3 $= 140 \times 140 \times 150$ grid cells. The size of the box is 5.560 Mm $\times$ 5.560 Mm $\times$ 2.25378 Mm. The $\tau = 1$ level is at a height of about 1.364 Mm from the bottom. The grid cells have a horizontal width of 40.0 km and a constant vertical extent of about 15.125 km.

Table 1 gives a compilation of runs with the additional models and new runs with model `d3t50g45mm00n04`.

Radiative flux at the top boundary

Figure 1 shows the total radiative output at the top in units of $\sigma T_{\rm eff}^4$ of the two solar models `d3gt57g44n59_B0` (red) and `d3gt57g44n59_v50` (green). For both models $s_{\rm inflow} = 1.7734 \times 10^9 =$ constant and both were computed with HLLMHD + PP. Both models show a similar and inconspicuous course in Frtop. However, in comparison to the larger solar models `job3DB0`, `job3dB0`, and `job3dRoe`, shown in Fig. 1 of part II, the amplitude of Frtop of the present models is larger and less regular. This may be due to the different areas over which Frtop is averaged but it is nevertheless surprising that the clear periodicity of the former solar models is basically absent here.

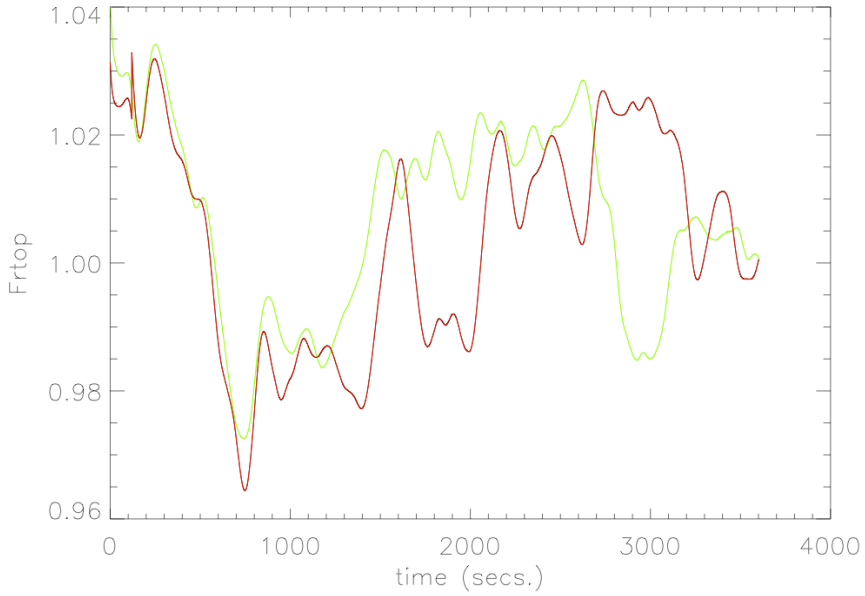

Figure 1: Bolometric radiative flux through the top boundary, Frtop, in units of $\sigma T_{\rm eff}^4$ as a function of time. Solar model in a box of n1 $\times$ n2 $\times$ n3 $= 140 \times 140 \times 150$ grid cells and dimensions 5.56 Mm $\times$ 5.56 Mm $\times$ 2.25 Mm. Red: $\mathbf{B} = 0$. Green: initial homogeneous vertical magnetic field of 50 G. Both computed with HLLMHD+PP.

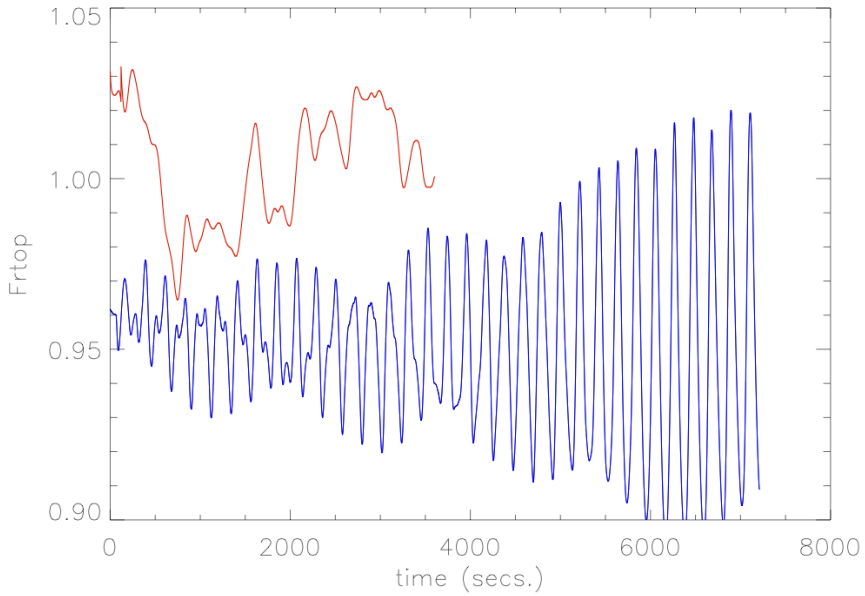

Figure 2: Bolometric radiative flux through the top boundary, Frtop, in units of $\sigma T_{\rm eff}^4$ as a function of time. Red: Sun, blue: model d3t40g45mm00n01. Both are computed with HLLMHD+PP and both have $\mathbf{B} = 0$.

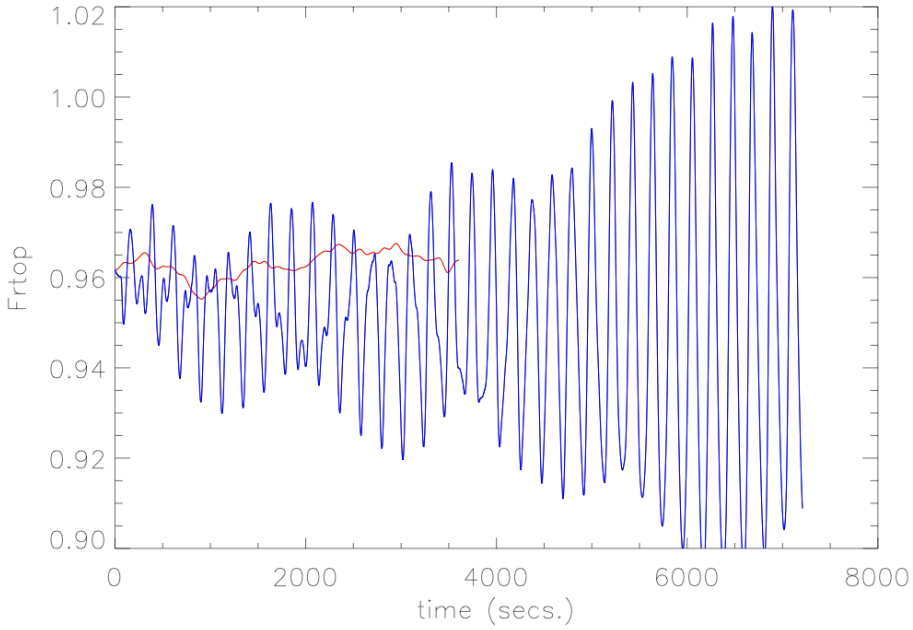

Figure 3: Bolometric radiative flux through the top boundary, Frtop, in units of $\sigma T_{\rm eff}^4$ as a function of time. Blue: HLLMHD+PP, red: Roe solver with VanLeer. Both runs with model d3t40g45mm00n01 and with $\mathbf{B} = 0$ for HLL and without magnetic field at all for Roe.

Figure 2 shows the total radiative output at the top in units of $\sigma T_{\rm eff}^4$ for the Sun (red) and for Model `d3t40g45mm00n01` (blue), both computed with HLLMHD+PP and $\mathbf{B} = 0$. The red curve in Fig. 2 is identical to the red curve in Fig. 1. Other than the fact that the $T_{\rm eff} = 4000$ K model is actually a little bit cooler than that nominal value, the following is immediately apparent. The stellar model shows a regular short period oscillation with increasing amplitude with time, which reaches $\approx 6\%$ vs. $\approx 3\%$ for the Sun. This is similar to but more pronounced than what we already found for the $T_{\rm eff} = 5000$ K model.

As in part II of this report for the $T_{\rm eff} = 5000$ K model, we now compare the radiative output of the $T_{\rm eff} = 4000$ K model once computed with HLLMHD+PP and $\mathbf{B} = 0$ and once with the Roe solver and van Leer reconstruction without magnetic field. The result is shown in Figure 3. As for the $T_{\rm eff} = 5000$ K model, the Roe solver does not show the large amplitude and regular oscillation of the model computed with the MHD solver. Thus, again, it seems that these strong oscillation are an artifact of the MHD solver. Moreover, here it seems that there is an instability at work, which lets the amplitude of the oscillation unabatedly increase with time.

For the $T_{\rm eff} = 5000$ K model we found in part II of this report that the introduction of a magnetic field did remove the oscillations. The fluctuations in the radiative output of the magnetic model was looking similar to the solar model or to the model computed with the Roe solver. Now, Fig. 4 shows the radiative flux through the top boundary in units of $\sigma T_{\rm eff}^4$ for the model with $T_{\rm eff} = 4000$ K, where the blue curve

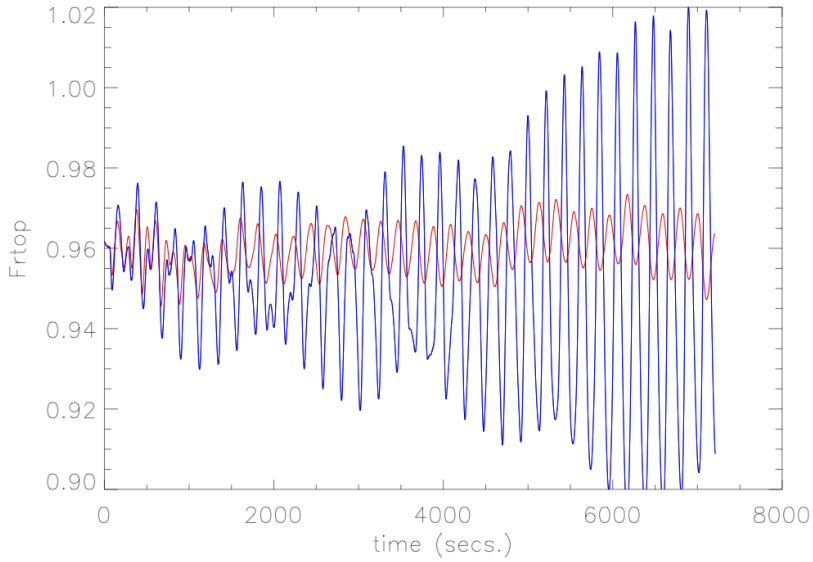

Figure 4: Radiative flux through the top boundary in units of $\sigma T_{\rm eff}^4$ as a function of time for the model with $T_{\rm eff} = 4000$ K. The blue curve refers to the model with $\mathbf{B} = 0$ computed with HLLMHD+PP, and the red curve to the model with an initial homogeneous vertical magnetic field of 50 G computed with HLLMHD+PP.

refers to the model with $\mathbf{B} = 0$ computed with HLLMHD+PP, and the red curve refers to the model with an initial homogeneous vertical magnetic field of 50 G, also computed with HLLMHD+PP.

Again, it seems that the magnetic field has a damping effect on the oscillations, however not as drastic as for the $T_{\rm eff} = 5000$ K model. Here, the model with magnetic field does oscillate with the same high frequency as the model with $\mathbf{B} = 0$ but with considerably lower amplitude and the amplitude does not increase with time and is, interestingly, shifted in phase by π with respect to the oscillation of the non-magnetic model.

Mass fluxes

Fig. 5 shows the horizontally averaged, vertical mass flux at the level of $\langle\tau\rangle = 1$ as a function of time for the solar model `job_d3gt57g44n59_B0` (red) and for the stellar model `job_d3t40g45mm00n01_B0` (blue) both with $\mathbf{B} = 0$ and computed with HLLMHD+PP.

As in Fig. 2, the stellar model oscillates with a larger amplitude than the solar model does. The solar model oscillates with a frequency of $\approx 5.17\,\mathrm{min} = 3.23\,\mathrm{mHz}$ while the stellar model oscillates with $\approx 3.52\,\mathrm{min} = 4.73\,\mathrm{mHz}$. The oscillation of the stellar model seems to consists of a superposition of two slightly different frequencies as two peaks gradually moves with respect to each other, which seems to produce a beat frequency.

Fig. 6 shows the horizontally averaged, vertical mass flux at the level of $\langle\tau\rangle = 1$

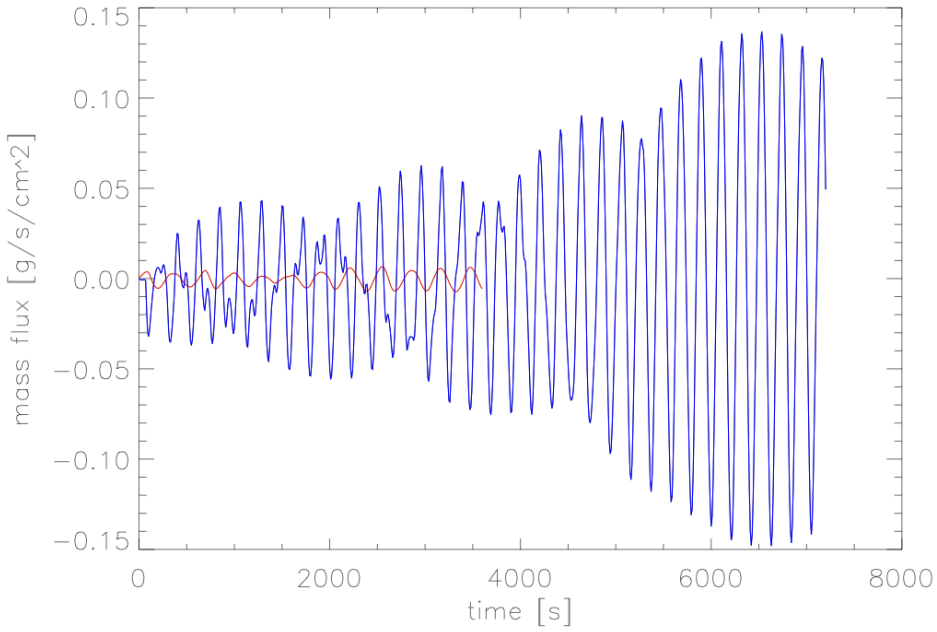

Figure 5: Horizontally averaged, vertical mass flux at the level of $\langle\tau\rangle = 1$ as a function of time. Red: Sun, blue: model d3t40g45mm00n01. Both are computed with HLLMHD+PP with $\mathbf{B} = 0$.

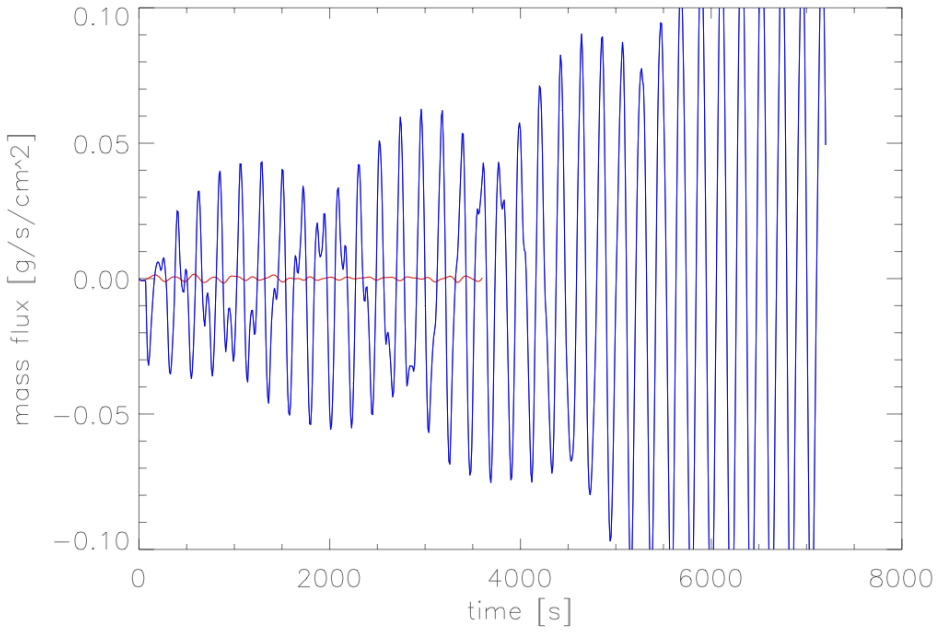

Figure 6: Horizontally averaged, verical mean mass flux at the level of $\langle\tau\rangle = 1$ as a function of time for model d3t40g45mm00n01. Blue: HLLMHD+PP and $\mathbf{B} = 0$. Red: Roe solver with VanLeer and no magnetic field.

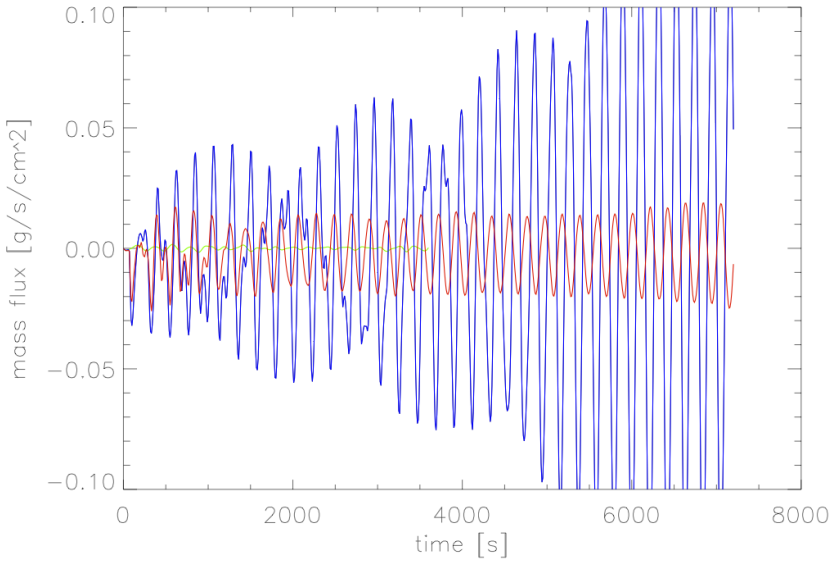

Figure 7: Horizontally averaged, vertical mass flux at a level of $\langle\tau\rangle = 1$ as a function of time for the model with $T_{\rm eff} = 5000$ K. The green curve refers to the model without magnetic field computed with the Roe solver, the blue curve to the model with $\mathbf{B} = 0$ computed with HLLMHD+PP, and the red curve to the model with an initial homogeneous vertical magnetic field of 50 G computed with HLLMHD+PP.

as a function of time for the stellar model `job_d3t40g45mm00n01`, once computed with HLLMHD+PP (blue) with $\mathbf{B} = 0$ and once with the Roe solver (red) without magnetic field. This figure confirms the result from Fig. 3 in that the Roe solver produces much smaller oscillations than the HLL solver does. Different from the $T_{\rm eff} = 5000$ K model (see Fig. 5 of part II), here the amplitude of the oscillation of the model computed with the Roe solver does not increase with time.

Finally, Fig. 7 shows the comparison of the horizontally averaged, vertical mass flux at the level of $\langle\tau\rangle = 1$ as a function of time for all models with $T_{\rm eff} = 4000$ K. The green curve refers to the model without magnetic field computed with the Roe solver, the blue curve to the model with $\mathbf{B} = 0$ computed with HLLMHD+PP, and the red curve to the model with an initial homogeneous vertical magnetic field of 50 G computed with HLLMHD+PP.

Different from the $T_{\rm eff} = 5000$ K model where the red curve did approach the amplitude and behaviour of the green curve (see Fig. 8 of part II), here, the magnetic model keeps oscillating although with a much smaller amplitude than the model with $\mathbf{B} = 0$ computed with HLLMHD+PP (blue curve). Also, the oscillation amplitude of the magnetic model seems not to grow with time but stays constant. Thus, similar to the $T_{\rm eff} = 5000$ K model, the introduction of the magnetic field has a damping effect. This is what we already stated in connection with Fig. 4.

Variation of the time integration

Following a suggestion by Bernd Freytag, we next have varied the time integration in order to check if this would have any influence on the oscillations. So far we were using the default time integration scheme when computing with the Roe solver. When computing with HLLMHD we have set `hdtimeintegrationscheme = Hancock` and the time step was allowed to vary with `c_courant`=0.7. For model `d3t50g45mm00n04` the time step varied between about 0.3 s and 0.45 s when integrating with the Roe solver. When using HLLMHD+PP, the time step varied between about 0.1 s and 0.4 s for the model with $\mathbf{B} = 0$ in phase with the mass-flux oscillation. For the model with initial homogeneous vertical magnetic field of 50 G, it varied between 0.1 s and 0.2 but stood most of the time very close to 0.2 s. The smaller time step is certainly due to the magnetic field, which limits the time step in the top part of the box. There, the maximum magnetic field strength is in the order of a few hundred Gauss and although occurring at different places, this maximal value is probably not varying much. Therefore the more or less constant time step.

It could this (the smaller and almost constant time step) be the reason which impedes oscillation of the magnetic model and not any 'damping' effect of the magnetic field. In order to test this hypothesis, we ran the model `d3t50g45mm00n04` with $\mathbf{B} = 0$ and HLLMMHD+PP, enforcing a constant time step of 0.1 s. The resulting vertical mass flux at the level of $\langle\tau\rangle = 1$ as a function of time is shown in Fig. 8.

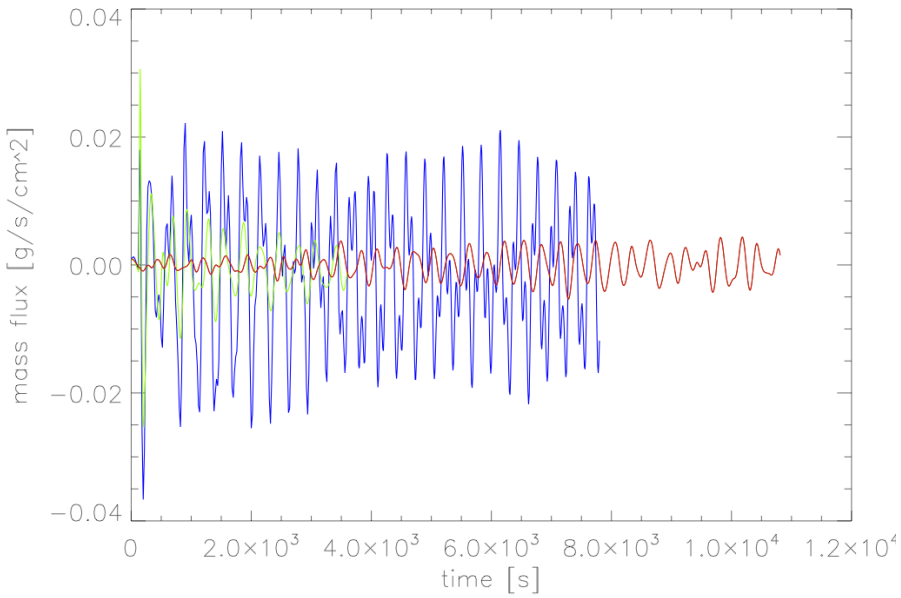

Figure 8: Horizontally averaged, verical mean mass flux at the level of $\langle\tau\rangle = 1$ as a function of time for model d3t50g45mm00n04. Red: Roe solver with VanLeer and no magnetic field, Blue: HLLMHD+PP and $\mathbf{B} = 0$, and Green: HLLMHD+PP and $\mathbf{B} = 0$ with a constant time step of 0.1 s.

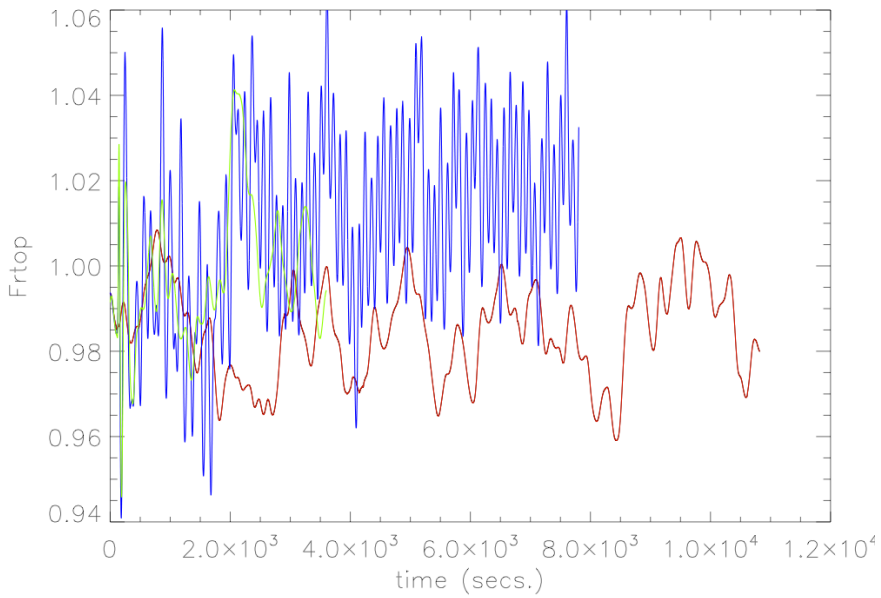

Figure 9: Bolometric radiative flux through the top boundary, Frtop, in units of $\sigma T_{\rm eff}^4$ as a function of time for model model d3t50g45mm00n04. Red: Roe solver with VanLeer, no magnetic field. Blue: HLLMHD+PP, $\mathbf{B} = 0$. Green: HLLMHD+PP, $\mathbf{B} = 0$, constant time step $\Delta t = 0.1$ s.

The red curve was obtained with the Roe solver wit a model without magnetic field, the blue curve with HLLMHD+PP and variable time step with a model with $\mathbf{B} = 0$, and the green curve again with HLLMHD+PP but with a constant time step of 0.1 s. The blue and the read curve are identical to the corresponding curves in Fig. 5 of part II of this report with the exception that the red curves carries now on until $t = 10818$ s. It does not further grow in amplitude as we earlier suspected from the first 7000 s. But most important, Fig. 8 shows that keeping the time step small and constant does get rid of the spurious large and growing oscillation with HLLMHD+PP. In Fact, the green curve approaches the behaviour and amplitude of the oscillation as computed with the Roe solver. This proves that something is wrong with the Hancock time integration. The solution should ideally not depend on the size of the time step as long as it is smaller than the maximum allowed time step given by the CLV condition. But obviously it depends on the time step size to a large degree.

Fig. 9 shows the bolometric radiative flux of the same three models as of Fig. 8. The green curve seems to follow the trend of the blue one but does not have the same high frequency oscillation but shows a fluctuation more similar to the red curve from the Roe solver.

Next we ran the same $T_{\rm eff} = 5000$ K model with $\mathbf{B} = 0$ and with the HLLMHD scheme and PP reconstruction but with `hdtimeintegrationscheme = RungeKutta2` leaving the time step variable again. It varied between 0.1 s and 0.45 s, which is similar to the variation with the Hancock integration scheme.

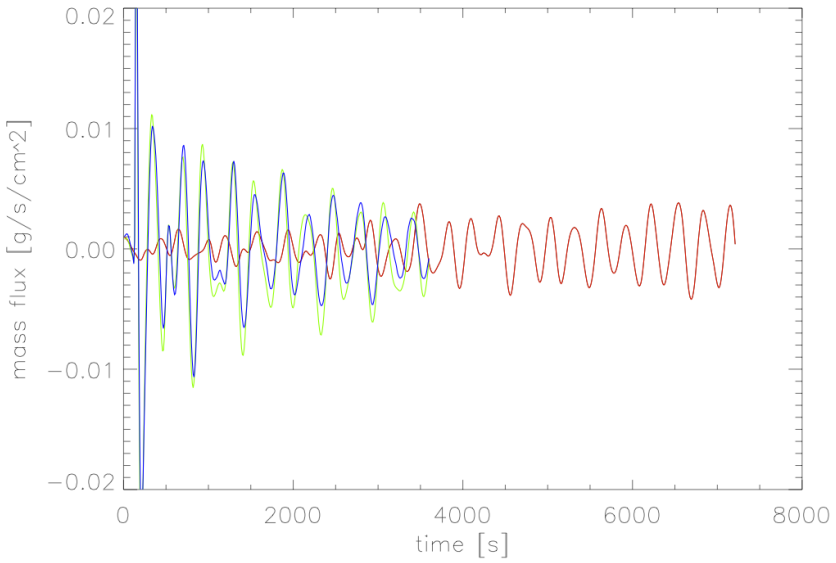

Figure 10: Horizontally averaged, vertical mean mass flux at the level of $\langle\tau\rangle = 1$ as a function of time for model d3t50g45mm00n04. Red: Roe solver with VanLeer and no magnetic field, Green: HLLMHD+PP and $\mathbf{B} = 0$ with constant time step $\Delta t = 0.1$ s, and Blue: HLLMHD+PP and $\mathbf{B} = 0$ with Runge Kutta time integration and variable time step.

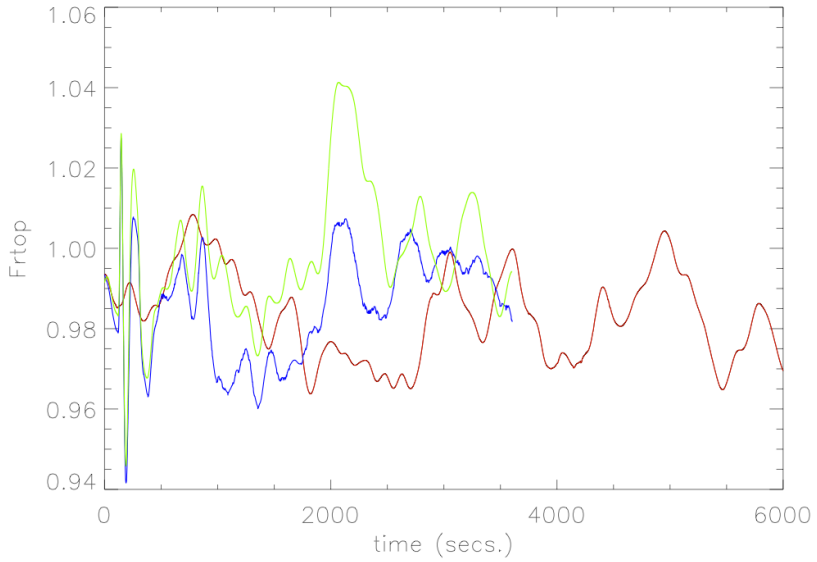

Figure 11: Bolometric radiative flux through the top boundary, Frtop, in units of $\sigma T_{\rm eff}^4$ as a function of time for model model d3t50g45mm00n04. Red: Roe solver with VanLeer, no magnetic field. Green: HLLMHD+PP, $\mathbf{B} = 0$, constant time step $\Delta t = 0.1$ s. Blue: HLLMHD+PP, $\mathbf{B} = 0$, Runge Kutta time integration.

Fig. 10 shows the horizontally averaged, vertical mean mass flux at the level of $\langle\tau\rangle = 1$ as a function of time. The red curve refers to the solution obtained with the Roe solver with VanLeer reconstruction and no magnetic field, the green curve to the solution with HLLMHD+PP and $\mathbf{B} = 0$ using a constant time step $\Delta t = 0.1$ s. The blue curve was obtained with HLLMHD+PP and $\mathbf{B} = 0$ with the Runge Kutta time integration with variable time step. This time, the blue and green curve follow each other very closely, as it should be, proving that the the time integration is stable for both cases. The Runge Kutta integration scheme shows a very regular and smooth oscillation.

Fig. 11 shows the bolometric radiative flux of the same three models as of Fig. 10. The green and the blue curve show the same trend although offset a bit with respect to each other. This time the blue curve (Runge Kutta) shows small-scale wiggles and is not very smooth.

Mean vertical mass flux as a function of heigth

In part II of this report we found spurious wiggles in plots of z, $\langle\rho v_z\rangle(z)$. We now want to check if they are still there when integratiing with a small constant time step or when integrating with the Runge Kutta scheme. Previously we found that the wiggles are still present for the models comprising a magnetic field but the mean mass flux asymptotically approached zero with height and the cell-boundary mass-flux stayed close to zero. We therefore can expect a similar behaviour for the above mentioned time integration schemes.

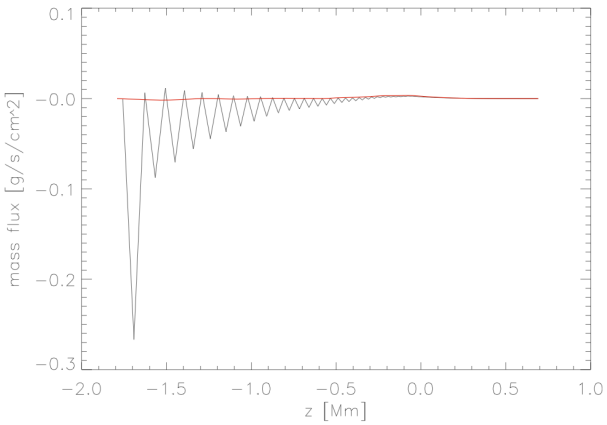

Figure 12: Horizontally averaged, vertical mass flux as a function of height z at $t = 2100$ s for the stellar simulation ($T_{\rm eff} = 5000$ K) with $\mathbf{B} = 0$ as computed with HLLMHD+PP and with constant small time step $\Delta t = 0.1$ s. The black curve is the cell centred mass flux (rhov3_xmean), while the red curve is the mass flux from the cell interfaces (rhovb_xmean).

This is indeed the case as one can see fron Figs. 12 and 13 with slight differences however. The cell interface fluxes stay much closer to zero for the cases with improved time integration and while this flux was forming an upper envelope for the

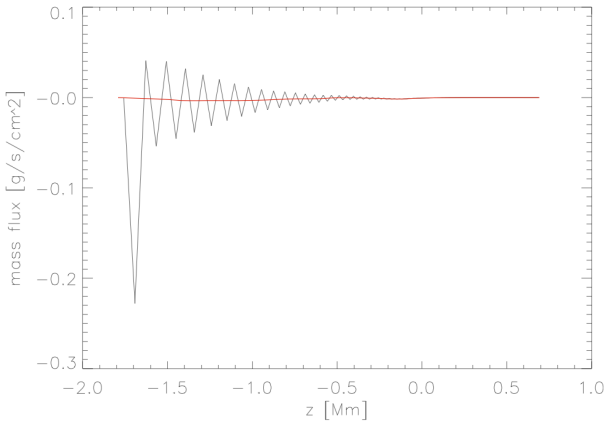

Figure 13: Horizontally averaged, vertical mass flux as a function of height z at $t = 2100$ s for the stellar simulation ($T_{\rm eff} = 5000$ K) with $\mathbf{B} = 0$ as computed with HLLMHD+PP and with Runge Kutta time integration. The black curve is the cell centred mass flux (rhov3_xmean), while the red curve is the mass flux from the cell interfaces (rhovb_xmean).

cell centred fluxes in the previous cases, in the simulation with Runge Kutta time integration, the mean value of the cell centred flux seems pretty accurately following the cell interface flux.

Bolometric intensity maps

Our final objective is to study small-scale magnetic flux concentrations in various stellar atmospheres. Despite of the various existing problems that still are with the MHD module, we here show a first rough comparison of a solar model with the $T_{\rm eff} = 5000$ K and the $T_{\rm eff} = 4000$ K model. In all three cases, the initial magnetic field was homogeneous, vertical of a strength of 50 G.

Figure 14 shows the solar model in the top panel, and the stellar models in the bottom row, where the left panel corresponds to the model with $T_{\rm eff} = 5000$ K and the right panel to the model with $T_{\rm eff} = 4000$ K. All three models clearly show magnetic flux concentrations as bright features located within intergranular lanes. These are not well resolved in all three cases, indicating that we need higher spatial resolution. In all three cases, the hot walls of the magnetic depression are conspicuously visible. This seems to be at variance with simulations from, e.g., the MuRam code, which shows a Gaussian-like distribution of brightness across magnetic flux sheets and not the double stripes especially well visible in the $T_{\rm eff} = 5000$ K model. This may be due to differences in the radiation transfer, in particular, short vs long characteristics.

The Sun shows this double layering less clearly than the cooler models, where magnetic flux concentrations seem to become wider. Most conspicuously, the shape of the bright features is changing from more elongated, sheet-like to more roundish, point-like when going from $T_{\rm eff} = 5000$ K to $T_{\rm eff} = 4000$ K.

It would be interesting to find out about the radiative energy budget of magnetic

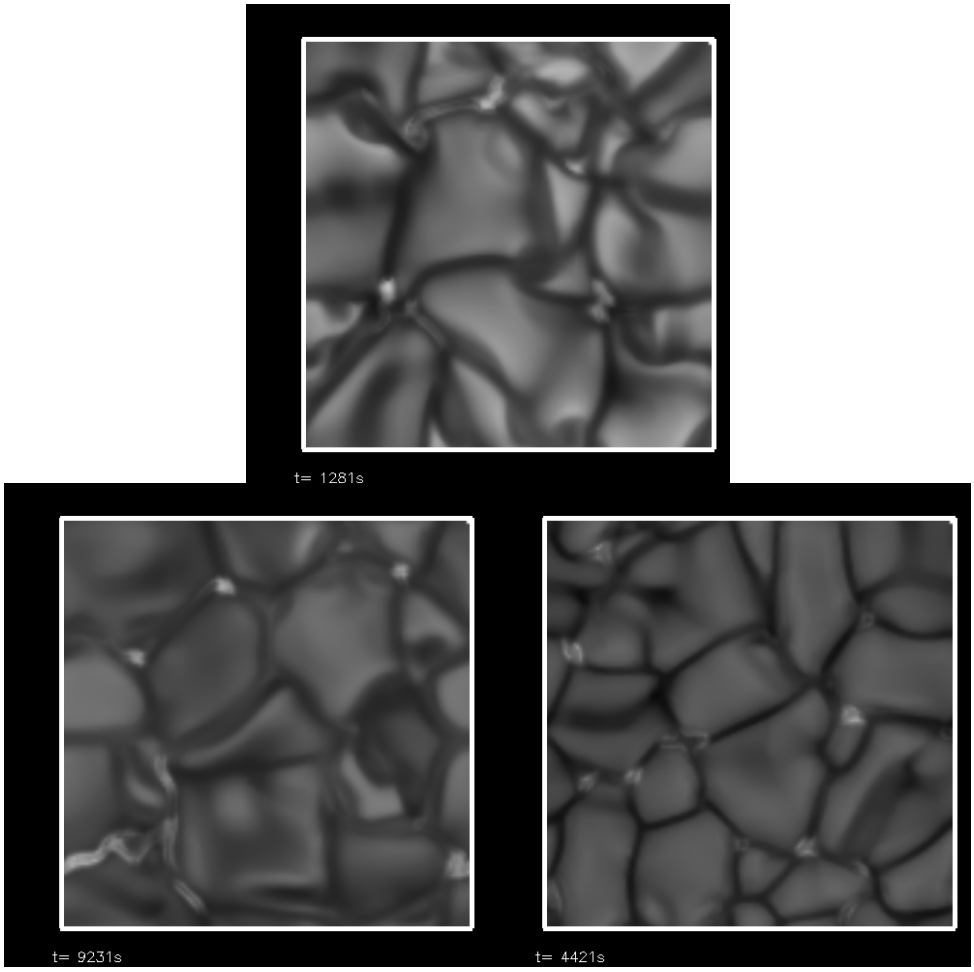

Figure 14: Bolometric intensity from the solar model(top), the $T_{\rm eff} = 5000$ K model (bottom, left), and the $T_{\rm eff} = 4000$ K model (bottom, right). All models computed with HLLMHD and PP reconstruction with Hancock time integration. All models have an initial homogeneous vertical magnetic field of strength 50 G. Snapshots were taken at times $t = 1291$ s, 9231 s, and 4421 s for the solar, the $T_{\rm eff} = 5000$ K, and the $T_{\rm eff} = 4000$ K model, respectively.

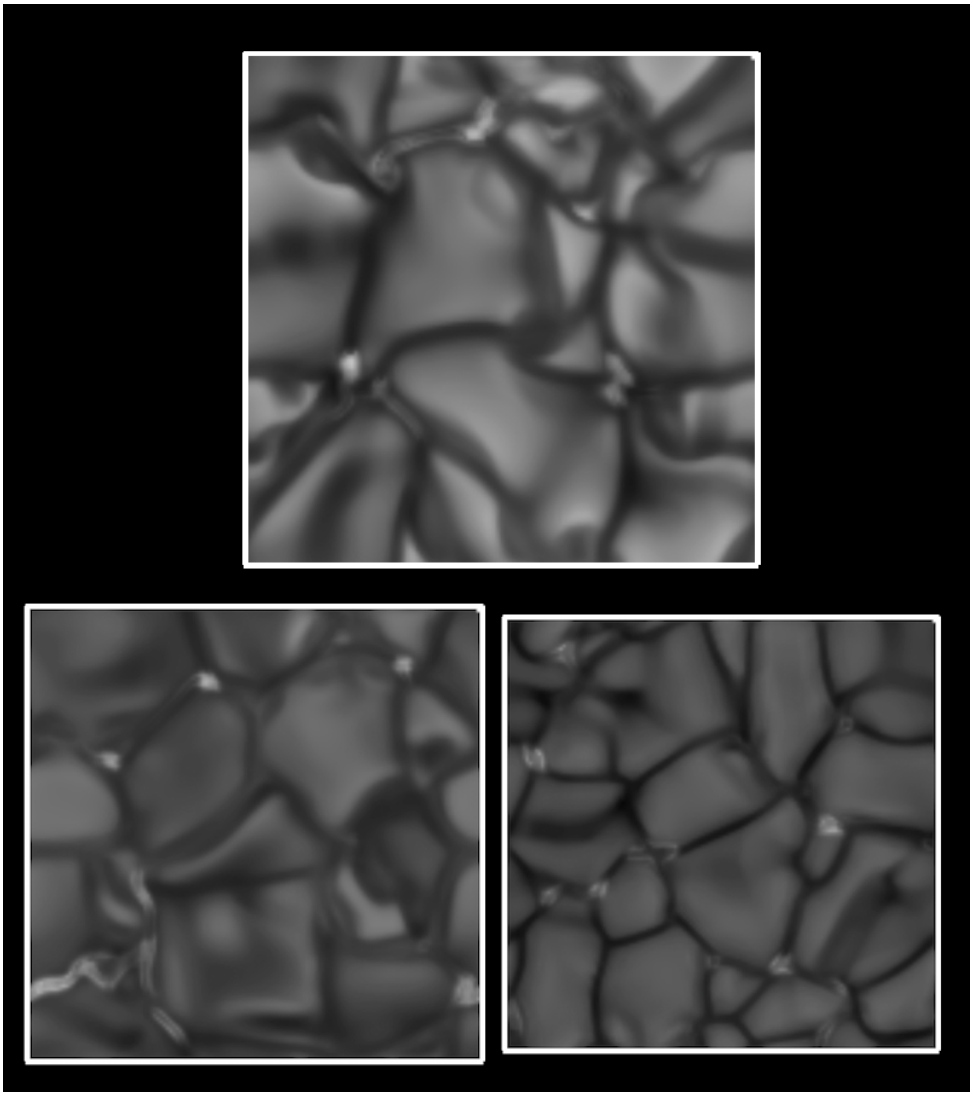

Figure 15: Like Fig. 14 but in correct size relation.

vs non-magnetic models for various stellar models. However, this is probably a challenging task, since Frtop is fluctuating considerably as one can see for example from Fig. 11. One would have to run an extremely long time series in order to obtain a reliable value for the mean radiative output, accurately enough to determine differences between magnetic and non-magnetic models. However, what could be done fairly straightforward is to construct a magnetic mask, say, based on a certain level of magnetic field strength. All the unmasked area, A_0 (with field strength below this level) would define a 'quiet star' region with the bolometric intensity $I_{\mathrm{bolo}\,0}$. The masked area, A_{mag} would define the intensity of the magnetic features, $I_{\mathrm{bolo\,mag}}$. Thus,

$$\frac{\langle A_0 I_{\mathrm{bolo}\,0} + A_{\mathrm{mag}} I_{\mathrm{bolo\,mag}} \rangle - \langle (A_0 + A_{\mathrm{mag}}) I_{\mathrm{bolo}\,0} \rangle}{\langle (A_0 + A_{\mathrm{mag}}) I_{\mathrm{bolo}\,0} \rangle}$$

defines the relative radiative surplus or radiative deficit of the magnetic model with respect to a hypothetically field-free model. The average $\langle ... \rangle$ is taken over a suitable time period. However, caution is indicated because this approach implicitly assumes that the unmasked area is not influenced by the magnetic field at all, viz., that $\langle I_{\mathrm{bolo}\,0} \rangle$ would reflect the mean intensity of a model without magnetic field.

Conclusions

We found that the Hancock time integration scheme is at the origin of the spurious oscillations in mass flux and luminosity of models cooler than the Sun. Remedy is provided by an artificial reduction of the time step (which is impractical) or switching to the Runge Kutta 2nd order time integration. In the past, it was mentioned in some email communications that Runge Kutta had not performed very well with MHD test problems. In fact we also observe small wiggles in the bolometric intensity as a function of time. So far, with the Runge Kutta scheme, we have only carried out simulations with the $T_{\mathrm{eff}} = 5000$ K model with $\mathbf{B} = 0$, not yet with models including a non-vanishing magnetic field and not yet with the $T_{\mathrm{eff}} = 4000$ K model. The Runge Kutta scheme has also moderated but by far not removed the wiggles in the cell-centred mass fluxes as a function of height. This problem is still with us and may be connected to the treatment of gravitation in the MHD module. In part II of this report, we found that the wiggles disappear (up to the lowermost grid layer) when switching to the van Leer reconstruction scheme so that we concluded that the wiggles occur in connection with PP. PP also produces strong wiggles (saw teeth) in the temperature (and other quantities) in the upper layers of magnetic models, mainly there where swirls are generated by the transverse movement of magnetic fields. In part I of this report we concluded that a hybrid reconstruction scheme (Bernd's Frankenstein?) might remedy this problem. So far we have not carried out any tests with the unsplit scheme that was recently implemented by Werner Schaffenberger into the MHD module.

Freiburg. i. Br., 18. 9. 2011